Desalination and Water Treatment
www.deswater.com
doi: 10.1080/19443994.2013.800324

52 (2014) 3367–3376
April

Taylor & Francis
Taylor & Francis Group

Adsorption of fluoride ions onto non-thermal plasma-modified CeO_2/Al_2O_3 composites

Tao Zhang[a,b], Qiurong Li[a,*], Zhenyu Mei[b], Haiyan Xiao[a], Hongxiao Lu[a], Yuming Zhou[b]

[a]*College of Environmental and Chemical Engineering, Hebei Key Laboratory of Applied Chemistry, Yanshan University, Qinhuangdao 066004, China*
Tel. +86 335 8387744; Fax: +86 335 8061569; email: liqiurong63@yahoo.cn
[b]*School of Chemistry and Chemical Engineering, Jiangsu Optoelectronic Functional Materials and Engineering Laboratory, Southeast University, Nanjing 211189, China*

Received 14 May 2012; Accepted 18 April 2013

ABSTRACT

The CeO_2/Al_2O_3 composites were synthesized by different synthesis methods and applied to remove excessive fluoride ions from water. The resulting materials were examined by scanning electron microscope (SEM), N_2 adsorption/desorption, and X-ray diffraction (XRD) analysis. In order to improve fluoride removal efficiency, non-thermal plasma (NTP) was used to modify the surface structure of the composites. Effects of calcination temperature, loading, solution pH, adsorption time, and coexisting anions on adsorption capacity were investigated in detail. The results indicated that the composites synthesized by co-precipitation method exhibit excellent removal efficiency in low-concentration fluoridated water. The appropriate adsorption capacity was achieved in the pH range of 3–10. The NTP-modified composites show high binding capacity for fluoride, where the maximum adsorption capacity of 37.0 mg/g was reached at the initial concentration of 120 mg/L. The kinetics of the fluoride adsorption processes were well described by the pseudo-second-order kinetic model. The equilibrium adsorption data, obtained from the experiment using adsorbents with and without NTP treatment, were analyzed by Redlich–Peterson, Temkin, and Dubinin–Radushkevich isotherm models. It was found that the Redlich–Peterson model provides the best correlation for the experimental data.

Keywords: CeO_2/Al_2O_3 composites; Adsorption; Non-thermal plasma; Fluoride removal

1. Introduction

Fluoride is a toxic element in source water with large-scale health effects upon prolonged drinking of water containing high fluoride content. The fluoride concentration recommended for potable water for human consumption is generally in the range of 0.5 mg/L–1.5 mg/L [1]. Excessive intake of fluoride may lead to dental fluorosis, skeletal fluorosis, and even crippling skeletal fluorosis [2]. Therefore, the elimination of fluoride from the source water is important to protect public health. Several techniques such as precipitation, adsorption, ion exchange, membrane processes, and electrodialysis have been evaluated for fluoride removal [3–6]. Among the various presented technologies, adsorption is one of the most efficient technologies for defluoridation. Large numbers of natural and low-cost adsorbents, namely activated zeolites, activated calcite, clays, red mud, activated carbons,

*Corresponding author.

modified activated carbons, bone char, and chitosan, have been used to remove excessive fluoride from water [6,7]; Many other adsorption materials such as hydrotalcite-like compound, rare earth metals, iron oxide, zirconium oxide, hydrous iron(III)–tin(IV) bimetal mixed oxide, and iron-zirconium hybrid oxide, which were synthesized by chemical method, were also used for defluoridation [6]. The final fluoride concentration of treated water must be controlled to a suitable value (~1.0 mg/L) according to the WHO guidelines. However, most of adsorbents have low removal efficiency in low-concentration fluoridated water. Therefore, an effective and inexpensive adsorbent with high fluoride removal efficiency is desirable.

Rare earth metals play an important role in the preparation of adsorbents for the removal of toxic ions from aqueous solutions. In recent years, considerable amount of work has been done on developing new rare earth metals adsorbent materials for fluoride removal, such as La^{3+}-impregnated cross-linked gelatin and Fe–Al–Ce trimetal oxide adsorbent [8,9]. The surface properties of adsorbents are important for adsorption, because the adsorption process is about specific interactions between the target molecules and the adsorbents' surface. In the past, growing attention has been focused on the new synthetic adsorbents or chemically modified adsorbents for defluoridation. However, little information has been reported in the literature about the surface modification of adsorbents. As a method of surface modification, the NTP surface modification takes advantages of high efficiency, simple operation, energy source saving and non-pollution, which play an important role in pollution prevention. The technique of NTP is more useful and effective than most chemical and thermal methods [10]. Though the NTP surface modification has obvious advantages over traditional chemical modification, as far as we know, there are still very few reports on the surface modification of adsorbents by NTP. The application of the NTP technique for adsorbent as surface modification, however, has not been well explored.

Thus, in this study, we report a novel adsorbent of CeO_2/Al_2O_3 composite for removing fluoride from water. The preparation conditions were optimized and the surface of adsorbents was modified by NTP. In addition, the characteristics of fluoride ions adsorption onto composites were investigated.

2. Materials and methods

2.1. Reagents

All the chemicals were of analytical grade and used as received without further purification. $Al_2(SO_4)_3{\cdot}18H_2O$ and $Ce(NO_3)_3{\cdot}6H_2O$ used in the present study were obtained from Tianjin Guangfu Fine Chemical Research Institute. NaF, $NaNO_3$, NaOH, HCl, $NH_3{\cdot}H_2O$, and $C_6H_5Na_3O_7{\cdot}2H_2O$ were purchased from Tianjin Windship Chemistry Technological Co., Ltd., γ-Al_2O_3 (215.8 m^2/g) was supplied by Xiamen University.

The total ionic strength adjustment buffer solution (TISAB) – 29.4 g $C_6H_5Na_3O_7{\cdot}2H_2O$ and 42.5 g $NaNO_3$ – were dissolved in 500 mL of deionized water; HCl was slowly dropped into the mixed solution until a pH of 5–6 was reached.

The fluoride ion stock solution, NaF, was calcined at 500°C for 1 h. 200 mg/L of fluoride ion stock solution was prepared by dried sodium fluoride and other fluoride test solutions were prepared by subsequent dilution of the stock solution.

2.2. Synthesis of adsorbents

The CeO_2/Al_2O_3 composites were synthesized by the co-precipitation method, impregnation–precipitation method, and solid-state reaction method, respectively.

2.2.1. Co-precipitation method

In a typical preparation, 0.002 mol $Ce(NO_3)_3{\cdot}6H_2O$ solution and 0.02 mol $Al_2(SO_4)_3{\cdot}18H_2O$ (Ce/Al = 1/20) were dissolved in 200 mL of deionized water, followed by the addition of aqueous ammonia until the pH of the solution reached 10.5. The resulting precipitates were filtered, washed with deionized water, and dried at 120°C in an air oven. Finally, the samples were calcined at the given temperatures for 4 h.

2.2.2. Impregnation–precipitation method

In the impregnation–precipitation method, γ-Al_2O_3 was impregnated with an aqueous solution containing $Ce(NO_3)_3{\cdot}6H_2O$ (Ce/Al = 1/20). The mixture was stirred at room temperature for 4 h while aqueous ammonia was added dropwise until the pH reached 10.5. The products were then filtered and washed with deionized water to ensure the complete removal of the physically adsorbed reactants. The filtrated samples were desiccated and then calcined at 250°C for 4 h.

2.2.3. Solid-state reaction method

The solid-state reaction method involved the mixing of γ-Al_2O_3 and $Ce(NO_3)_3{\cdot}6H_2O$ as starting materials; the mixed solid powder with Ce/Al of 1/20

was ground for 30 min and then calcined at the given temperatures for 4 h.

2.3. Surface modification of the CeO_2/Al_2O_3 composites

The CeO_2/Al_2O_3 composites were modified by NTP (Plasma generator CTP-2000 K) before calcination (pre-treatment) and after calcination (post treatment); the power of the NTP treatment for the samples was 60 W and the time duration of treatment was 10 min. In isotherms and kinetics studies, pre-treated composites have been employed to remove fluoride from aqueous solution.

2.4. Adsorption experiments

Batch adsorption studies were carried out as follows: 0.1 g of the adsorbent was added in 50 mL (dose, 2 g/L) of sodium fluoride at the initial concentration of 20–120 mg/L. The time required to reach equilibrium as determined in equilibrium studies was 24 h, and the time for kinetic studies was more than 1.5 h. The fluoride ions remaining in the test solution were measured with a fluoride ion selective meter (pF–1). The adsorption capacity was calculated from the following equation:

$$q_e = (C_0 - C_e)V/m \quad (1)$$

where q_e is the adsorption capacity (mg/g) at equilibrium, C_0 and C_e are the initial and the equilibrium fluoride concentration (mg/L), respectively, V is the volume (mL) of solution, and m is the weight (g) of the adsorbent used.

2.5. Adsorbent characterization

The morphology of the raw and NTP-modified composites was investigated by use of a Philips XL30 electron microscope. The surface and porosity of the samples were measured by a surface area analyzer (NOVA-4000e). The crystal phase of the adsorbent samples was studied by X-ray diffraction (XRD) (TTR-III).

3. Results and discussion

3.1. Preparation optimization

3.1.1. Effect of synthesis method

In order to establish the optimum conditions for the synthesis method, the prepared samples were added to 50 mL of fluoride solution at the initial concentration of 20 mg/L. The adsorption capacities of three different adsorbents are shown in Fig. 1. It can be seen from the results that the synthesis method has a significant effect on the adsorption capacity, and the maximum adsorption capacity was observed by adsorbents prepared by the co-precipitation method. The adsorbents are showing excellent fluoride removal efficiency of 94.66% and overcome the drawbacks associated with the conventional adsorbents. The excellent adsorption capacity may be attributed to the high dispersion of cerium with the co-precipitation method. It is expected to be a new defluoridation adsorbent that can be used for naturally fluoridated water treatment. Therefore, the adsorbents synthesized by co-precipitation method have been chosen for further studies.

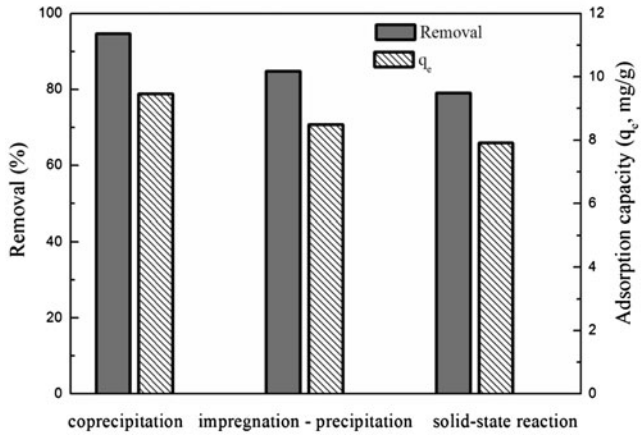

Fig. 1. Comparison of removal efficiency of adsorbents by different synthesis methods (conditions: adsorption time, 24 h; initial concentration, 20 mg/L; does, 2 g/L; and pH, 6–7).

3.1.2. Effect of cerium loading

It has been known that molar ratio of cerium to aluminum (Ce/Al) is an important parameter for adsorption. The optimization of synthesis of adsorbent has been done by varying the Ce/Al ratio as 1/40, 2/40, 4/40, and 6/40. In order to study the effect of cerium loading on fluoride removal, γ-Al_2O_3 and CeO_2 were also used for adsorption. The results of the fluoride adsorption capacity are presented in Fig. 2. It can be found that the adsorption capacity of CeO_2/Al_2O_3 composites is far greater than that of γ-Al_2O_3 and CeO_2. It is also noticed that the adsorption capacity of fluoride increased with increasing cerium loading. Increasing the cerium loading resulted in the maximum adsorption capacity of fluoride increasing from 28.83 mg/g to 34.86 mg/g. Hence, it can be concluded that the active phase of the composites was cerium. On further increasing of cerium loading, the

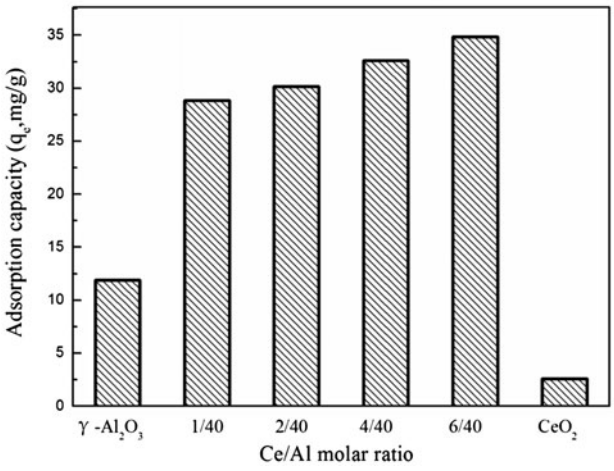

Fig. 2. Adsorption capacity affected by loading (conditions: adsorption time, 24 h; initial concentration, 100 mg/L; does, 2 g/L; and pH, 6–7).

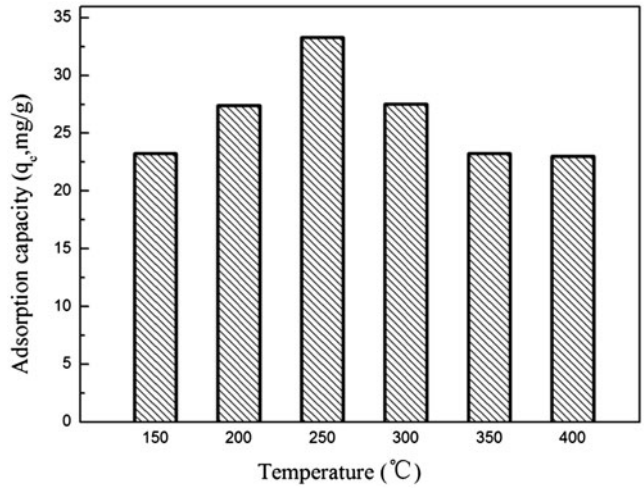

Fig. 3. Adsorption capacity affected by different calcination temperature (conditions: adsorption time, 24 h; initial concentration, 100 mg/L; does, 2 g/L; and pH, 6–7).

adsorption capacity increased very slowly. Hence, the adsorbent materials with molar ratio of 2/40 have been chosen for further experiments.

3.1.3. Effect of thermal treatment

Thermal pre-treatment of adsorbents can influence their adsorption ability, as previous studies have reported [9]. Hence, in the present study, the fluoride removal was studied at different calcination temperatures and the results are shown in Fig. 3. The results showed that the fluoride adsorption capacity had been enhanced with increasing of calcination temperatures from 150℃ to 250℃. Thereafter, the adsorption capacity of adsorbents had declined with increasing calcination temperature from 250℃ to 400℃. The optimal calcination temperature was 250℃, at which higher fluoride removal efficiency could be reached. The increased adsorption capacity may be attributed to the changed specific surface area and porosity of the composites. On the other hand, NH_4^+ might exist in the rare earth metal surfaces; as cerium has a strong affinity to NH_4^+, the NH_4^+ might reduce the adsorption sites. The NH_4^+ would leave the surface of composites with the increasing temperatures. Therefore, the surface of CeO_2/Al_2O_3 composites was activated at the appropriate temperature. Less fluoride adsorption at higher temperature was attributed to the decomposition of surface –OH.

3.2. Characterizations of the adsorbent

The surface morphologies of raw and NTP-modified composites were observed by SEM. As shown in Fig. 4A and B, the lumpy particles of the two samples have similar sizes, even though the samples are irregular in shape and surface. Compared to the morphology of raw composites, the surfaces of NTP-modified composites changed greatly. Sheet structures can be found at the surface of NTP-modified adsorbents, indicating that the surface structure has been changed by NTP modification. The active species, such as high-energy electrons and reactive radicals, generated in plasma can change the upper layers of the composites during NTP treatment, which is called the "etching effect" [11,12]. The layer structures on the surface of the lumpy particles will lead to the increase of specific surface area and pore structure. It can be presumed that the adsorption on NTP-modified composites is more favorable.

The XRD patterns of samples prepared at different calcination temperatures are displayed in Fig. 5. All the peaks were AlO(OH) peaks (JCPDS No. 49-0133), and no characteristic peaks of cerium compounds were found. It was indicated that ceria was highly dispersed into alumina with the co-precipitation method. The reflections of synthesized products show broad and asymmetric peaks, implying that the products are composed of amorphous mixed oxides with poor crystallinity. Several studies reported that non-crystalline hydroxides can be used for defluoridation, such as "amorphous Fe/Al mixed hydroxides" [13]. Additionally, a broad peak appeared at around 28˚, which may be attributed to the peak overlapping of the decomposed hydroxides. The hydroxides could be decomposed into mixed oxides at higher calcination temperatures. The surface –OH of composites was lost, resulting in the decrease of adsorption sites.

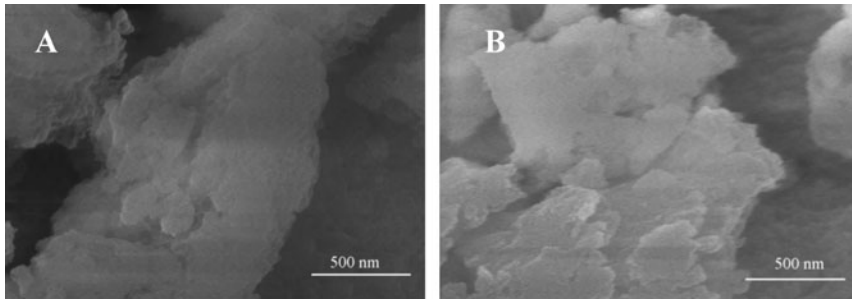

Fig. 4. SEM micrographs of raw and NTP-modified CeO_2/Al_2O_3 composites.

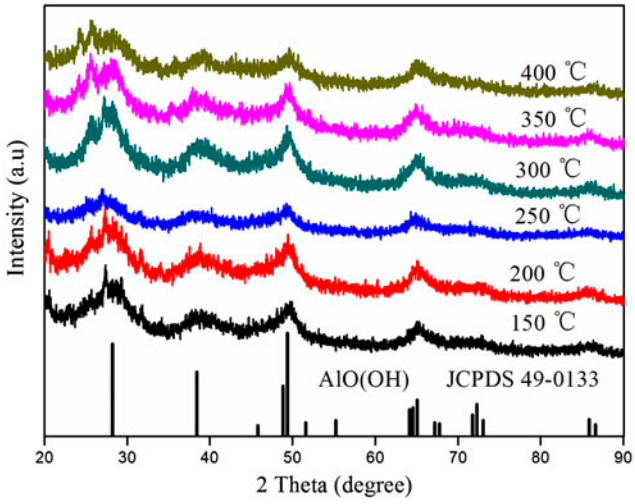

Fig. 5. XRD patterns of adsorbents calcined at different temperatures.

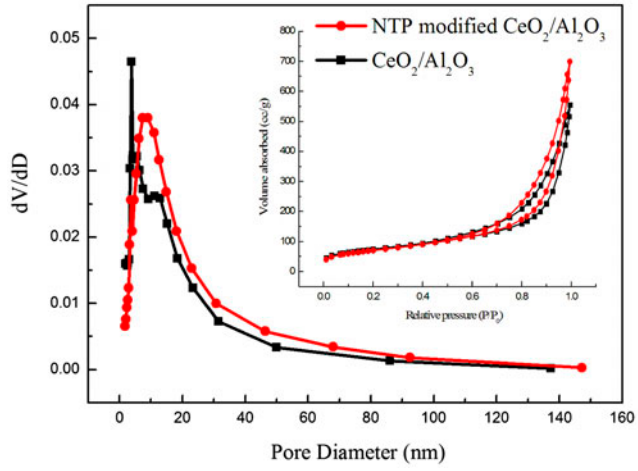

Fig. 6. BJH pore-size distributions and N_2 adsorption–desorption isotherms (inset) of raw and NTP-modified CeO_2/Al_2O_3 composites.

The adsorption capacity of an adsorbent often follows the pore structure and total surface area, since there are usually more available active binding sites on a material with higher surface area [14]. The surface and porosity of the samples were characterized by N_2 adsorption–desorption analysis. Fig. 6 shows the pore-size distribution and nitrogen adsorption–desorption isotherms of raw and NTP-modified composites. The corresponding pore-size distributions indicate that the pore structures are basically mesoporous with pore sizes predominantly less than 50 nm, with average pore diameters of ~3.5 nm (raw composites) and ~9.0 nm (NTP-modified composites). The increased pore diameter of NTP-modified composites may be attributed to the etching effect of NTP treatment. The isotherms (inset of Fig. 6) present the characteristic features of a type IV with a broad H_3 hysteresis loops, indicating the presence of mesopores as well as macropores in morphology analysis. The BET specific surface areas of raw and NTP-modified composites were measured to be 255.5 m^2/g and 266.1 m^2/g, respectively. The large surface areas provide more adsorption sites for fluoride adsorption, making the adsorption process more efficient.

Fig. 7 shows the TG–DTA curves of the as-prepared sample. The TG curve clearly shows that the weight of composites decreased with increasing calcination temperature. The weight loss was attributed to the removal of –OH groups and water molecules. As can be seen in Fig. 7, two endothermic peaks were observed in the DTA curve. The first one from room temperature to 320˚C was due to the removal of surface-adsorbed and crystal water. Hence, the thermal-activated composites with increased adsorption sites are favorable for fluoride adsorption. The second one with a strong exothermic peak centered at 455˚C was attributed to the dehydroxylation of the composites. Hence, the structure of composites was changed at a higher calcination temperature. There are no phase changes in the XRD patterns at calcination temperatures below 400˚C, which is in agreement with the thermal analysis.

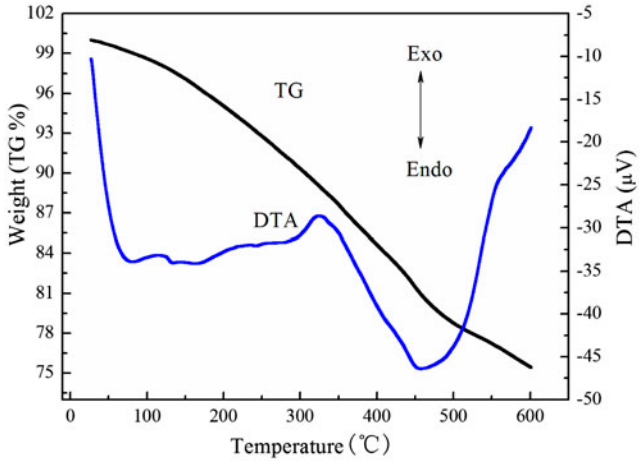

Fig. 7. TG–DTA curves of as-prepared sample.

3.3. Non-thermal plasma modification of CeO_2/Al_2O_3 composites

Removal of fluoride through adsorption is highly dependent on the surface properties of adsorbents. In order to alter the surface properties of the adsorbent, the adsorbents were modified by NTP before calcination and after calcination, respectively. The results are shown in Fig. 8; it is apparent that the NTP-modified adsorbents have higher adsorption capacity than original composites. The fluoride removal capacity increased from 24.1 mg/g to 37.0 mg/g by the adsorbents pre-treatment, compared with original composites at the initial concentration of 120 mg/L. As we know, adsorption is an interfacial reaction and chemisorption is a monolayer adsorption [15]. The active species generated in plasma can activate the upper molecular layers of the interface [16,17]. Thus, the active phase of CeO_2/Al_2O_3 composites may be well dispersed. The results also suggested that the increased amount of adsorption sites produced is due to the surface of NTP-treated CeO_2/Al_2O_3 composites which were activated. The increased adsorption capacity of plasma-treated adsorbents was inferred that the activation energy of adsorption was reduced [15]. This factor might explain the increased adsorption capacities. Hence, the NTP technique is very useful for fluoride removal.

3.4. Batch sorption behaviors

3.4.1. Effect of solution pH

The fluoride solution was studied by adjusting the pH from 2 to 13 using NaOH and HCl solutions under an initial concentration of 100 mg/L. The results are shown in Fig. 9; the optimum pH for the uptake of fluoride appeared at pH 3–10. The maximum adsorption capacity was observed at neutral pH, whereas in both acidic and alkaline solution there was a decline in the adsorption capacity. The fluoride adsorption capacity decreased drastically at higher pH values, which was attributed to the competition for adsorption sites by excessive amounts of hydroxide ions [6]. On the other hand, with the increase of solution pH, adsorbent surface by the positive charge changed into negative charge; an electrostatic repulsion, therefore, existed between the adsorbent and fluoride ions, which resulted in the decrease of fluoride adsorption capacity. When the pH was lower

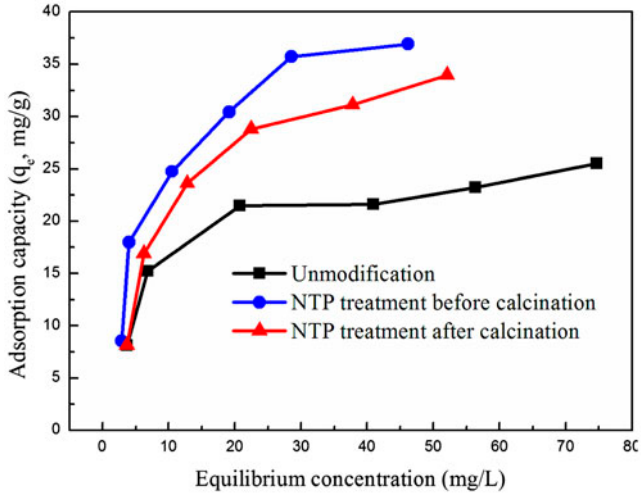

Fig. 8. Adsorption capacity affected by NTP treatment (conditions: adsorption time, 24 h; initial concentration, 20–120 mg/L; does, 2 g/L; and pH, 6–7).

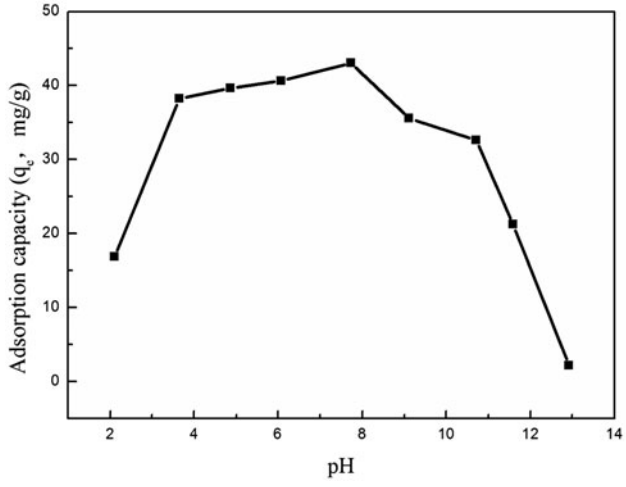

Fig. 9. Adsorption capacity affected by solution pH (conditions: adsorption time, 24 h; initial concentration, 100 mg/L; and does, 2 g/L).

than 3, the concentration of acid affects the adsorption process through the dissociation of adsorbents' surface functional groups (–OH) [6]. Less fluoride adsorption was attributed to the loss of surface adsorption sites.

3.4.2. Effect of adsorption time

Adsorption time is an important parameter that controls the adsorption process related to optimum parameter conditions in the application of the adsorbents for water treatment systems. Fig. 10 shows adsorption capacity of the adsorbents at low fluoride concentration as a function of contact time at the temperature 25°C. As time increased, the removal rate also increased, and then gradually approached a constant value. It was clear that the equilibrium of fluoride adsorption was achieved with a treatment time of 1.5 h. After that there was no further increase in the adsorption. The fluoride removal rate recorded a maximum percentage of 99. Since the composites show excellent fluoride removal efficiency, they are expected to separate fluoride from low-concentration fluoridated water.

3.4.3. Effect of co-anions

The influence of coexisting ions, such as HPO_4^{2-}, CO_3^{2-}, SO_4^{2-}, NO_3^{-}, $C_2O_4^{2-}$, and Cl^{-}, on fluoride adsorption was studied. This study assessed fluoride adsorption behavior in initial fluoride concentration of 100 mg/L, and the same concentration of other anions were mixed together. The results are shown in Fig. 11; it can be seen that fluoride adsorption capacity in the presence of anions decreased in the order: $Cl^{-} < NO_3^{-} < SO_4^{2-} < CO_3^{2-} < C_2O_4^{2-} < HPO_4^{2-}$. The phosphate and oxalate are insoluble salts in Cerium salt; the sorption process was altered in the presence of HPO_4^{2-} and $C_2O_4^{2-}$, which could be partly attributed to the strong competition between coexisting ions and fluoride on active adsorption sites. An electrostatic attraction, therefore, existed between the absorbent and divalent anions, which led to the decrease of the adsorption capacity in the presence of CO_3^{2-} and SO_4^{2-}.

3.5. Kinetics of adsorption

The kinetics of adsorption can be described using several models, such as the pseudo-first-order model, pseudo-second-order model, and intraparticle diffusion model.

The pseudo-first-order kinetic model, called the Lagergren model, has been widely used to predict the adsorption kinetics [18–20]:

$$\ln(q_e - q_t) = \ln q_e - k_1 t \quad (2)$$

The values of k_1 can be obtained from the slope of the plot of $\ln(q_e - q_t)$ vs. t.

The pseudo-second-order equation based on the equilibrium adsorption is expressed as [21–23]:

$$q_t = \frac{k_2 q_e^2 t}{1 + k_2 q_e t} \quad (3)$$

or equivalently,

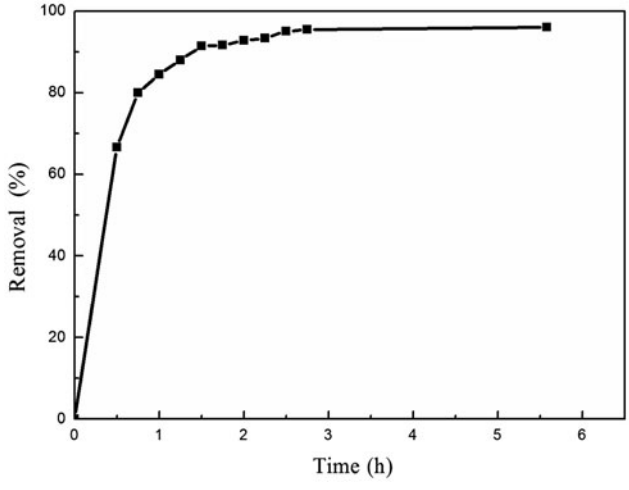

Fig. 10. Effect of time on the removal rate of fluoride (conditions: initial concentration, 20 mg/L; does, 2 g/L; and pH, 6–7).

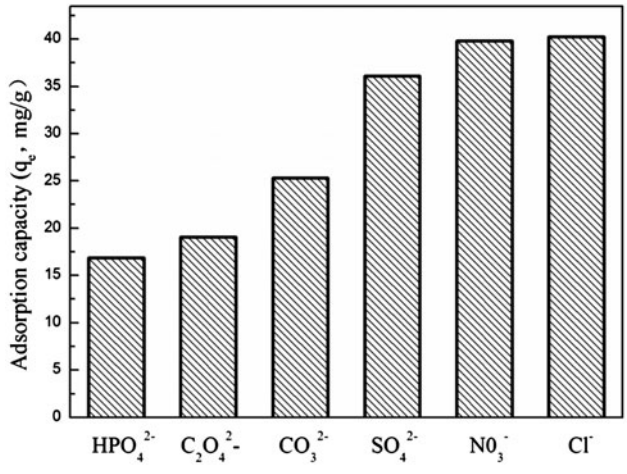

Fig. 11. Adsorption capacity affected by the solution coexisting anions (conditions: adsorption time, 24 h; initial concentration, 100 mg/L; does, 2 g/L; and pH, 6–7).

$$\frac{t}{q_t} = \frac{1}{k_2 q_e^2} + \frac{t}{q_e} \quad (4)$$

Eq. (4) shows that the plot of t/q_t vs. t should be a line with slope and intercept of $1/q_e$ and $1/(k_2 q_e^2)$, respectively.

In the process of adsorption of fluoride ions on adsorbents, there is the possibility of intraparticle diffusion [24–27], which could be described as:

$$q_t = k_p t^{1/2} + C \quad (5)$$

According to Eq. (5), if the adsorption mechanism follows the intraparticle diffusion processes, a plot of q_t vs. $t^{1/2}$ should be a straight line with a slope k_p and intercept C.

Table 1 shows the correlation coefficient R^2 of different kinetic models; the result shows that the pseudo-second-order model is indicative of a chemisorption mechanism, which fits the experimental data much better than the pseudo-first-order model and intraparticle diffusion model. The correlation coefficient value of intraparticle diffusion model was relatively small, which shows that the process of diffusion was not the rate-determining step of fluoride adsorption.

Fig. 12 represents the plot of pseudo-second-order kinetic model for adsorption of fluoride at the concentration of 20 mg/L, 40 mg/L, and 60 mg/L. The q_e and k_2 can be calculated from the slope and intercept. The correlation coefficient for the second-order-kinetic model approaches 1, indicating the applicability of the pseudo-second-order kinetic model to describe the adsorption of fluoride onto composites. It also means that the mechanism of fluoride adsorption was controlled by chemisorption or ion exchange. It seems from Table 1 that the rate constant k_2 of fluoride increases with NTP modification, which is due to the increase in the number of available adsorption sites because of NTP treatment. It could also be seen that the rate constants decrease with increasing fluoride ions concentration; the same trend has also been reported in the removal of fluoride ions by hydrous iron(III)–tin(IV) bimetal mixed oxide [28], which may be due to the decreasing number of adsorption sites at higher concentration of fluoride ions.

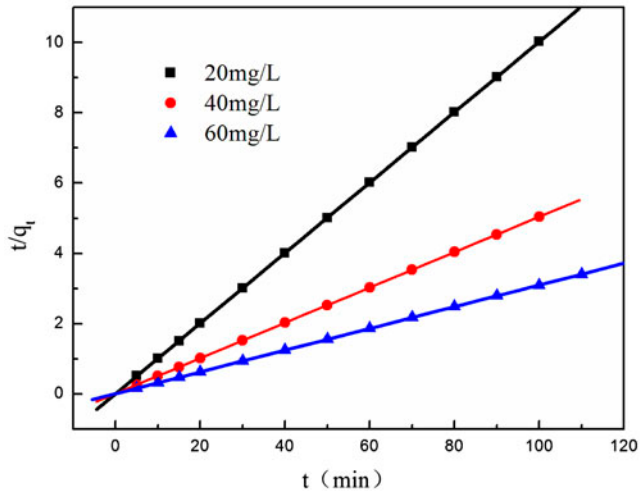

Fig. 12. Pseudo-second-order kinetics for adsorption of fluoride onto CeO_2/Al_2O_3 composites at different concentrations.

3.6. Adsorption isotherms

Fig. 8 shows the isotherms of fluoride adsorption on pristine and NTP-modified CeO_2/Al_2O_3 composites. The results of the kinetic study indicate that the mechanism of fluoride ion adsorption was mainly by chemisorption. In order to confirm the fit the isotherm model for the chemisorption system, it is necessary to analyze the data using the monolayer model or adsorbent–adsorbate interactions model, such as

Table 1
Kinetic parameters for adsorption of fluoride onto CeO_2/Al_2O_3 composites

	Concentration (mg/L)	Pseudo-first-order	Pseudo-second-order		Intraparticle diffusion
		R^2	R^2	k_2 (g/mg min)	R^2
Unmodified	20	0.7062	0.9997	0.3665	0.1191
	40	0.9553	1	0.2528	0.5707
	60	0.9434	0.9994	0.1214	0.3824
NTP-modified	20	0.7582	0.9996	1.4520	0.4323
	40	0.7536	0.9999	0.2348	0.6893
	60	0.7407	0.9992	0.1498	0.7429

Table 2
Equilibrium constants for isotherm models

		Unmodified	NTP-modified
Temkin	A	3.648	1.338
	B	5.094	9.797
	R^2	0.9621	0.9779
Redlich–Peterson	g	0.7926	0.6769
	R^2	0.9972	0.9975
Dubinin–Radushkevich	q_m (mg/g)	23.00	33.70
	E (J/mol)	407.3	450.8
	R^2	0.9780	0.9542

Redlich–Peterson, Temkin, and Dubinin–Radushkevich (D–R) isotherm models [29–33].

The Redlich–Peterson equation is widely used as a compromise between Langmuir and Freündlich systems. The Redlich–Peterson equation is expressed as:

$$q_e = \frac{\alpha C_e}{1 + \beta C_e g} \tag{6}$$

and can be linearized as:

$$\ln\left(\frac{\alpha C_e}{q_e - 1}\right) = g \ln C_e + \ln \beta \tag{7}$$

The Temkin isotherm contains a factor that explicitly takes into account the adsorbent–adsorbate interaction. The adsorption heat of all the molecules in the layer would decrease linearly with coverage due to adsorbent–adsorbate interactions, which could be described as:

$$q_e = A + B \ln C_e \tag{8}$$

The D–R isotherm model was used to describe the character of adsorption process, whether it is physical or chemical [31,32]. The linearized D–R equation is written as follows:

$$\ln q_e = \ln q_{max} - \beta\varepsilon^2 \tag{9}$$

β is a model constant related to the free sorption energy, ε (Polanyi potential) is equal to RT $\ln(1 + 1/C_e)$, and the mean free energy of sorption (E) is equal to $-1/\sqrt{2\beta}$.

The correlation coefficient R^2 and equilibrium constants of isotherm models are listed in Table 2. For Redlich–Peterson model, the correlation coefficients are closer to 1. This suggests that the adsorption isotherms of fluoride onto CeO_2/Al_2O_3 composites can be represented better by the Redlich–Peterson model. Generally speaking, the chemisorption is monolayer adsorption and physisorption is multilayer adsorption [34,35]. The Langmuir equation is valid for monolayer sorption, while the Freündlich isotherm model has been proposed as a multilayer sorption. For $g = 1$, the Redlich–Peterson model can be converted into the Langmuir form, but the values of g calculated from experimental data are not 1; it might cause the electrostatic interaction or hydrogen bond between the adsorbent surfaces and fluoride ions. As can be seen in Table 2, the D–R model did not fit the experimental data satisfactorily. Thus, it is inferred that fluoride adsorption onto composites was not a multilayer adsorption.

4. Conclusion

The CeO_2/Al_2O_3 composites have been synthesized by a simple chemical co-precipitation method. By varying the Ce/Al molar ratios and calcination temperature, we got the optimum conditions of synthesizing adsorbents: Ce/Al mol ratio of 1/20 and calcination temperature of 250˚C. The NTP-modified adsorbents have a higher adsorption capacity than pristine composites. The optimum fluoride adsorption was observed at pH 3–10. The coexisting anions have little effect on the fluoride adsorption, except HPO_4^{2-} and $C_2O_4^{2-}$. The kinetics of adsorption of fluoride adsorption was well represented by the pseudo-second-order kinetic model, and the adsorption isotherms of adsorption were best fitted by the Redlich–Peterson model. From the kinetics and isotherms analysis, the fluoride adsorption mechanism by composites was mainly governed by chemisorption.

Acknowledgments

The authors would like to thank Jenna Shorten and anonymous reviewers for their suggestions, which have significantly improved the quality of this manuscript. We are also thankful for the financial

support from the Natural Science Foundation of China (No. 51077013) and Fund Project for Transformation of Scientific and Technological Achievements of Jiangsu Province of China (No. BA2011086).

References

[1] M.M. Naim, A.A. Moneer, G.F. El-Said, Defluoridation of commercial and analar sodium fluoride solutions without using additives by batch electrocoagulation–flotation technique, Desalin. Water Treat. 44 (2012) 110–117.
[2] M. Mohapatra, T. Padhi, S. Anand, B.K. Mishra, CTAB mediated Mg-doped nano Fe_2O_3: Synthesis, characterization, and fluoride adsorption behavior, Desalin. Water Treat. 50 (2012) 376–386.
[3] N. Drouiche, S. Aoudj, H. Lounici, H. Mahmoudi, N. Ghaffour, M.F.A. Goosen, Development of an empirical model for fluoride removal from photovoltaic wastewater by electrocoagulation process, Desalin. Water Treat. 29 (2011) 96–102.
[4] N. Drouiche, H. Lounici, M. Drouiche, N. Mameri, N. Ghaffour, Removal of fluoride from photovoltaic wastewater by electrocoagulation and products characteristics, Desalin. Water Treat. 7 (2009) 236–241.
[5] T. Zhang, Q. Li, H. Xiao, H. Lu, Y. Zhou, Synthesis of Li–Al layered double hydroxides (LDHs) for efficient fluoride removal, Ind. Eng. Chem. Res. 51 (2012) 11490–11498.
[6] A. Bhatnagar, E. Kumar, M. Sillanpää, Fluoride removal from water by adsorption: A review, Chem. Eng. J. 171 (2011) 811–840.
[7] Y. Vijaya, S.R. Popuri, G.S. Reddy, A. Krishnaiah, Development and characterization of chitosan coated biopolymer sorbent for the removal of fluoride ion from aqueous solutions, Desalin. Water Treat. 25 (2011) 159–169.
[8] Y. Zhou, C. Yu, Y. Shan, Adsorption of fluoride from aqueous solution on La^{3+}-impregnated cross-linked gelatin, Sep. Purif. Technol. 36 (2004) 89–94.
[9] X. Wu, Y. Zhang, X. Dou, M. Yang, Fluoride removal performance of a novel Fe–Al–Ce trimetal oxide adsorbent, Chemosphere 69 (2007) 1758–1764.
[10] E. Alkan, E. Kir, L. Oksuz, Plasma modification of the anion-exchange membrane and its influence on fluoride removal from water, Sep. Purif. Technol. 61 (2008) 455–460.
[11] L. Yang, J. Chen, Y. Guo, Z. Zhang, Surface modification of a biomedical polyethylene terephthalate (PET) by air plasma, Appl. Surf. Sci. 255 (2009) 4446–4451.
[12] C. Wang, J.-r. Chen, R. Li, Studies on surface modification of poly(tetrafluoroethylene) film by remote and direct Ar plasma, Appl. Surf. Sci. 254 (2008) 2882–2888.
[13] M.G. Sujana, G. Soma, N. Vasumathi, S. Anand, Studies on fluoride adsorption capacities of amorphous Fe/Al mixed hydroxides from aqueous solutions, J. Fluorine Chem. 130 (2009) 749–754.
[14] N.D. Hutson, S.A. Speakman, E.A. Payzant, Structural effects on the high temperature adsorption of CO_2 on a synthetic hydrotalcite, Chem. Mater. 16 (2004) 4135–4143.
[15] T. Zhang, Q.R. Li, Y. Liu, Y.L. Duan, W.Y. Zhang, Equilibrium and kinetics studies of fluoride ions adsorption on CeO_2/Al_2O_3 composites pretreated with non-thermal plasma, Chem. Eng. J. 168 (2011) 665–671.
[16] D. Sun, G.K. Stylios, Fabric surface properties affected by low temperature plasma treatment, J. Mater. Process. Technol. 173 (2006) 172–177.
[17] F. Arefi-Khonsari, J. Kurdi, M. Tatoulian, J. Amouroux, On plasma processing of polymers and the stability of the surface properties for enhanced adhesion to metals, Surf. Coat. Technol. 142–144 (2001) 437–448.
[18] S.K. Swain, T. Padhi, T. Patnaik, R.K. Patel, U. Jha, R.K. Dey, Kinetics and thermodynamics of fluoride removal using cerium-impregnated chitosan, Desalin. Water Treat. 13 (2010) 369–381.
[19] P.K. Annamalai, C. Pochat-Bohatier, D. Bouyer, C.-L. Li, A. Deratani, D.-M. Wang, Kinetics of mass transfer during vapour-induced phase separation (VIPS) process and its influence on poly-(vinylidene fluoride) (PVDF) membrane structure and surface morphology, Desalin. Water Treat. 34 (2011) 204–210.
[20] Y. Vijaya, M. Venkata Subbaiah, A. Subba Reddy, A. Krishnaiah, Equilibrium and kinetic studies of fluoride adsorption by chitosan coated perlite, Desalin. Water Treat. 20 (2010) 272–280.
[21] Y.S. Ho, G. McKay, Pseudo-second order model for sorption processes, Process. Biochem. 34 (1999) 451–465.
[22] T. Zhang, Y. Zhou, M. He, Y. Zhu, X. Bu, Y. Wang, Biomimetic fabrication of hierarchically structured LDHs/ZnO composites for the separation of bovine serum albumin, Chem. Eng. J. 219 (2013) 278–285.
[23] I.V. Soares, E.G. Vieira, N.L.D. Filho, A.C. Bastos, N.C. da Silva, E.F. Garcia, L.J.A. Lima, Adsorption of heavy metal ions and epoxidation catalysis using a new polyhedral oligomeric silsesquioxane, Chem. Eng. J. 218 (2013) 405–414.
[24] J.-q. Chen, Z.-j. Hu, R. Ji, Removal of carbofuran from aqueous solution by orange peel, Desalin. Water Treat. 49 (2012) 106–114.
[25] V. Mishra, C.B. Majumder, V.K. Agarwal, Sorption of Zn(II) ion onto the surface of activated carbon derived from eucalyptus bark saw dust from industrial wastewater: Isotherm, kinetics, mechanistic modeling, and thermodynamics, Desalin. Water Treat. 46 (2012) 332–351.
[26] S.C. Panchangam, K. Janakiraman, Sorptive removal of color from aqueous coffee and tea infusions, Desalin. Water Treat. 50 (2012) 338–347.
[27] P. Kumar, R. Agnihotri, K.L. Wasewar, H. Uslu, C. Yoo, Status of adsorptive removal of dye from textile industry effluent, Desalin. Water Treat. 50 (2012) 226–244.
[28] K. Biswas, K. Gupta, U.C. Ghosh, Adsorption of fluoride by hydrous iron(III)–tin(IV) bimetal mixed oxide from the aqueous solutions, Chem. Eng. J. 149 (2009) 196–206.
[29] H.A. Panahi, H.B. Sadeghi, N. Farahmandnejad, A.R. Badr, E. Moniri, Removal of cobalt from human serum and environmental samples by adsorption using Amberlite XAD-2–salicylic acid–iminodiacetic acid, Desalin. Water Treat. 46 (2012) 244–255.
[30] L. Huang, Y. Sun, Q. Yue, Q. Yue, L. Li, B. Gao, Adsorption of Cd(II) on lotus stalks-derived activated carbon: Batch and column studies, Desalin. Water Treat. 41 (2012) 122–130.
[31] S. Çoruh, F. Geyikçi, Adsorption of copper (II) ions on montmorillonite and sepiolite clays: Equilibrium and kinetic studies, Desalin. Water Treat. 45 (2012) 351–360.
[32] K.M. Doke, M. Yusufi, R.D. Joseph, E.M. Khan, Biosorption of hexavalent chromium onto wood apple shell: Equilibrium, kinetic and thermodynamic studies, Desalin. Water Treat. 50 (2012) 170–179.
[33] A.O. Alade, O.S. Amuda, A.O. Ibrahim, Isothermal studies of adsorption of acenaphthene from aqueous solution onto activated carbon produced from rice (Oryza sativa) husk, Desalin. Water Treat. 46 (2012) 87–95.
[34] J. Chen, R. Qu, Y. Zhang, C. Sun, C. Wang, C. Ji, P. Yin, H. Chen, Y. Niu, Preparation of silica gel supported amidoxime adsorbents for selective adsorption of Hg(II) from aqueous solution, Chem. Eng. J. 209 (2012) 235–244.
[35] X.-H. Guan, J. Wang, C.C. Chusuei, Removal of arsenic from water using granular ferric hydroxide: Macroscopic and microscopic studies, J. Hazard. Mater. 156 (2008) 178–185.